

Tracing non-equilibrium plasma dynamics on the attosecond timescale in small clusters

Ulf Saalmann¹, Ionuț Georgescu and Jan M Rost

Max Planck Institute for the Physics of Complex Systems,
Nöthnitzer Straße 38, 01187 Dresden, Germany
E-mail: us@pks.mpg.de

New Journal of Physics **10** (2008) 025014 (10pp)

Received 25 September 2007

Published 29 February 2008

Online at <http://www.njp.org/>

doi:10.1088/1367-2630/10/2/025014

Abstract. It is shown by microscopic calculations that the energy absorption of a rare-gas cluster from a vacuum-ultraviolet (VUV) pulse can be traced with time-delayed extreme-ultraviolet (XUV) attosecond probe pulses by measuring the kinetic energy of the electrons detached by the probe pulse. By means of this scheme we demonstrate that, for pump pulses as short as one femtosecond, the charging of the cluster proceeds during the formation of an electronic nano-plasma inside the cluster. Using moderate harmonics for the VUV and high harmonics for the XUV pulse from the same near-infrared laser source, this scheme with well defined time delays between pump and probe pulses should be experimentally realizable. Going to even shorter pulse durations we predict that pump and probe pulses of about 250 attoseconds can induce and monitor non-equilibrium dynamics of the nano-plasma.

¹ Author to whom any correspondence should be addressed.

Contents

1. Introduction	2
2. Theoretical method	3
3. Observation of transient cluster charging	3
4. Instantaneous cluster ionization: formation, equilibration and relaxation of a nano-plasma	6
5. Creating and monitoring of non-equilibrium plasmas in clusters with attosecond pump–probe pulses	8
6. Summary	9
References	10

1. Introduction

The production, characterization and application of ultrashort attosecond laser pulses is undergoing breathtaking development. With isolated pulses already technically possible [1] attosecond pulses or pulse trains are presently used in combination with a strong near-infrared (NIR) pulse from which the attosecond pulses were generated in the first place. Although the strong NIR pulse in many cases modifies the target, it conveniently provides a clock which indicates at which time t the attosecond pulse acted on an electron, since the final momentum $\vec{p}_{\text{final}} = \vec{p}_{\text{excited}} + e\vec{A}(t)$ of an ionized electron contains as drift momentum the vector potential $\vec{A}(t)$ of the NIR field at time t and is therefore streaked by the NIR pulse [2, 3].

We have proposed a different pump–probe scheme: a vacuum-ultraviolet (VUV) pulse (about 100 fs duration and 20 eV frequency) excites a rare-gas cluster, and the evolution of the electron dynamics is traced by a time-delayed attosecond pulse. While such a combination promises to deliver insight into fast dissipative multi-electron dynamics in the cluster [4], it is still experimentally out of reach. However, one can generate the VUV pulse from harmonics of a strong NIR pulse and combine it with an attosecond pulse. The price to pay is that the VUV pulse will be relatively short, namely a few femtoseconds which are almost a factor 100 shorter than before [4]. Here, we explore this new scenario which, moreover, gives rise to new phenomena in the cluster dynamics as detailed below.

Rare-gas clusters are ideal to explore ways of probing ultrafast dynamics which are quite different from atoms or small molecules: most importantly, due to the large number of nuclear and electronic degrees of freedom and the high density of the probed matter, the electron dynamics is transient and dissipative in character. It is transient because redistribution of energy among the many degrees of freedom occurs on a microscopic timescale and it is dissipative because it is virtually impossible to measure all degrees of freedom after a long time in the energy domain. Furthermore, clusters allow one to control the electron dynamics much better through a suitable combination of the light pulse (appropriate length, intensity and wavelength) and the size of the cluster [5], than is possible in the condensed phase.

After introducing our approach in section 2, we analyze in section 3 the dynamics of small argon clusters with 13 and 55 atoms under a VUV pulse of a few femtoseconds and an attosecond probe pulse, focusing on mapping out the charging of the cluster which happens dominantly during the rising part of the VUV pulse. This scenario extrapolates the one studied before [4] to shorter excitation times. We find an interesting new phenomenon in a small

time window at the crossover between instant and delayed ionization. To understand this phenomenon we replace the pump pulse in section 4 with a sudden excitation of electrons. It turns out that their subsequent dynamics is that of a strongly-coupled non-equilibrium plasma [6] which oscillates between kinetic and potential energy with the plasma frequency, indeed explaining the crossover found in section 3 as the remainder of this non-equilibrium dynamics when excited and probed with relatively long pulses. Consequently, we demonstrate in section 5 that one can indeed observe this non-equilibrium plasma dynamics if attosecond pump and probe pulses are used, by tracing the potential energy in form of the charging of the cluster, as described before. We summarize our results in section 6.

2. Theoretical method

In order to simulate the dynamics of electrons and cluster ions upon excitation by VUV laser pulses we have used a hybrid approach which combines quantum-mechanical absorption rates for bound electrons and classical propagation of the photo-ionized electrons. The approach is similar to those successfully applied to cluster dynamics driven by NIR laser pulses [5]. Details of the adaption to the VUV regime have been published elsewhere [7]. Therefore we will only briefly review the main steps and assumptions here. Bound electrons may absorb photons according to the known photo-absorption rates [8], i.e. there is a certain probability for absorption within a given time step. Due to this statistical feature one has to average over an ensemble of realizations, where each realization is a deterministic ionization sequence and the ensemble, containing typically about 100 realizations, is in accordance with the absorption rate. After their ‘creation’ the electrons are propagated classically in the field of the laser and all previously generated electrons and ions. In contrast to photo-absorption of isolated atoms, electrons are not necessarily free but may be trapped in the cluster potential, i.e. by the attractive Coulomb potential of neighboring ions. These electrons are called quasi-free electrons. Whereas the classical propagation is straightforward, it is challenging to properly describe the impact of the electrons and ions on further ionization of bound electrons. We have developed a method for calculating the photo-ionization rates in clusters which takes into account localization of electrons around a particular ion [7]. This ‘classical recombination’ is of minor importance for the short pulses studied here but becomes relevant for longer pulses [4] as produced by free-electron-laser sources.

3. Observation of transient cluster charging

We will study the transient charging of small clusters using a pump–probe scenario proposed recently [4]. The clusters are excited by a VUV pump pulse, which lasts—in contrast to our previous study—only for a few femtoseconds, and probed with time-delayed attosecond extreme-ultraviolet (XUV) pulses. The instantaneous charge at time t , measured with respect to the VUV pump pulse, is imprinted in the final kinetic energy of the electron ionized by the XUV pulse. Slower electrons indicate higher charges. By subtracting the average kinetic energy at the detector from the photon energy we obtain the average ionization potential, which is converted into an average charge by interpolating between the ionization potentials of isolated Ar ions. In our simulations the detector is replaced by long expansion times, which ensures that the XUV photo-electrons are well separated from the cluster, typically by more than 250 cluster radii.

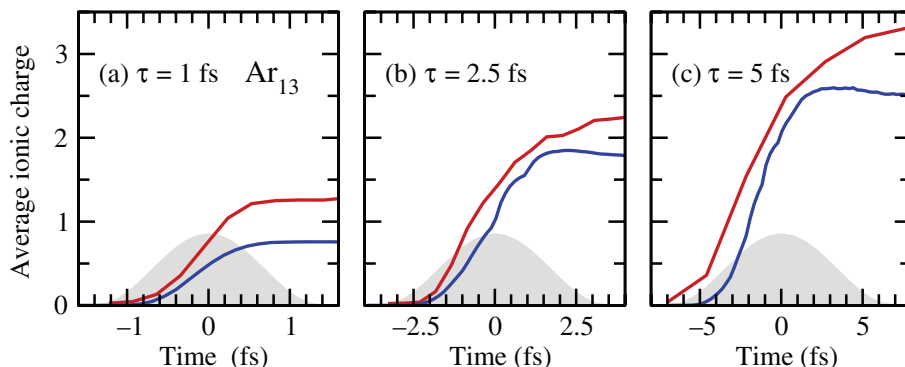


Figure 1. Average charge of ions in an Ar₁₃ cluster induced by laser pulses (gray shaded areas) with three different pulse lengths $\tau = 1, 2.5$ and 5 fs and the central frequency $\hbar\omega = 20$ eV and the same intensity $I = 7 \times 10^{13}$ W cm⁻². We compare the ionic charge (blue lines) due to photo-ionization by the pump pulse with the charge probed by the kinetic energy of electrons released by the delayed attosecond pulse (red lines), see text for details.

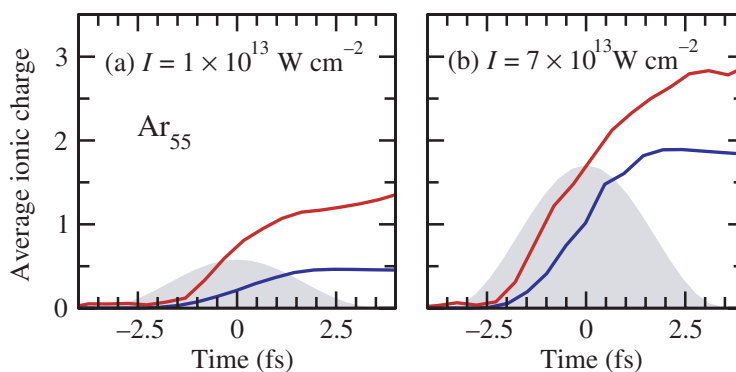


Figure 2. Same quantities as in figure 1, but for an Ar₅₅ cluster and laser pulses of the same duration $\tau = 2.5$ fs and different intensities, $I = 1 \times 10^{13}$ W cm⁻² and 7×10^{13} W cm⁻², respectively.

The parameters chosen for the pump and probe pulses are motivated by their experimental availability [9]. Both pulses are most easily obtained from filtering of (different) harmonics from a driving NIR laser. Besides a flexible duration of the pump pulse, most importantly, this enables an accurate setting of the delay of the probing XUV pulse. The intensity of the probe pulse is of minor importance. On average less than one electron is photo-ionized per pulse due to the low cross-sections for XUV frequencies. A lower intensity can be compensated by a higher repetition rate.

Figures 1 and 2 show the charging for Ar₁₃ and Ar₅₅ clusters, respectively. In both cases the pump frequency was $\hbar\omega = 20$ eV. For the smaller cluster we kept the intensity I constant and changed the pulse duration τ ; for the larger cluster we did it vice versa. Photo-absorption due to the pump pulses leads to excitation of electrons either directly into the continuum or—due to the increasing space charge—into the cluster. In either of the cases the electron is lost from the mother ion and the ionic charge increases. The average charges of all cluster ions, as extracted

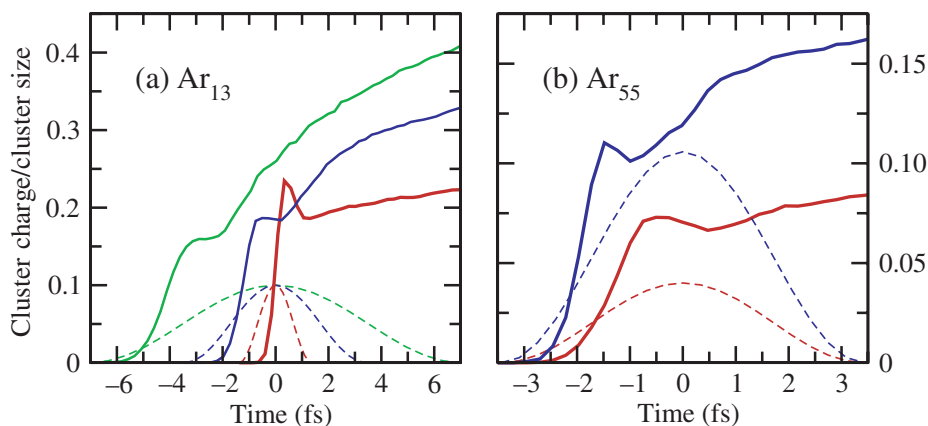


Figure 3. Total charge of the cluster, i.e. number of electrons with positive energy, divided by the cluster size. Left panel: cluster and laser pulse parameters as in figure 1, right panel: as in figure 2. The envelopes of the electric fields for the corresponding pump pulses are shown by dashed lines.

directly from the simulation, are shown by the blue lines in figures 1 and 2. The maximum of the ionization rates (strongest increase) shifts to earlier times if the pulse is made longer (as from figures 1(a) to (c)) or if the intensity is increased (as from figures 2(a) to (b)). This is due to the depletion of the atoms in the cluster. It becomes relevant for average ionic charges larger than one, which is the case in figures 1(b), (c) and 2(b). For the ‘long’ pulse with $\tau = 5$ fs one observes localization or recombination of electrons which results in a decreased charge at the falling edge of the pulse, i.e. for times $t > 2.5$ fs. During the pulse we do not find noticeable localization.

The ionic charge as obtained from the attosecond probe pulses ($\hbar\omega = 150$ eV, $I = 10^{15}$ W cm $^{-2}$ and $\tau = 500$ as) is shown by red lines in figures 1 and 2. In this case the horizontal axis corresponds to the time delay of the probe pulses. Although the probing does not resemble the charging process perfectly for all cases, it performs particularly well when the charging is strongest, namely slightly before the pulse maximum. There are basically three reasons for the apparent deviations. (i) The space charge reduces the kinetic energy of the probing electrons and results in an overestimation of the ion charges. This effect is more important for Ar $_{55}$ as compared to Ar $_{13}$ because of the larger cluster charge. (ii) Evaporation of quasi-free electrons increases the space charge as well. This effect becomes relevant only late in time, in our examples, after the pump pulse is over, see the deviation of both quantities in figure 1(c). (iii) For either very short (figure 1(a)) or very weak (figure 2(a)) pulses both quantities show an (almost linearly) increasing divergence already at early times. Note the difference to the other cases, where both curves are largely parallel during the initial charging. The increasing divergence is due to the low number of electrons captured by the cluster potential. Since the cluster does not host a plasma which would allow for screening of the ionic charges, the increasing space charge is directly imprinted in the probing signal.

Since the total cluster charge influences the probing signal, it is presented in figure 3 as a function of time for the cases considered above. It is defined by the number of electrons with positive energy $E > 0$. The energy of the j th electron (mass m and charge $-e$) with velocity \vec{v}_j

is given by

$$E_j = \frac{m\vec{v}_j^2}{2} - \sum_{i(\neq j)}^{\text{all}} \frac{q_i e^2}{|\vec{r}_i - \vec{r}_j|}, \quad (1)$$

whereby the sum runs over all (except the electron itself) charged particles with charge $q_i e$ at the position \vec{r}_i . In order to make Ar₁₃ and Ar₅₅ comparable the cluster charge is normalized to the number of cluster atoms. In all cases the charging of the cluster shows clearly two phases, namely fast direct charging early in the pulse and slow evaporation towards the end of the pulse and later on. Whereas for the longer pulses and Ar₁₃, cf green and blue lines in figure 3(a), these phases are separated by a plateau, in the other cases the cluster charge even drops after a maximum before evaporation sets in. Comparison with figures 1 and 2 reveals that this ‘overshooting’ is connected with a high photo-absorption rate, i.e. a large number of atoms becomes ionized within a short time interval. This is either due to a quick rise² of the laser intensity, as for the 1 fs pulse, or due to a large number of available atoms, as for Ar₅₅. The plateau, or even the overshooting of the charge at the crossover from direct ionization to evaporation, is most easily understood if one considers the limit of instant ionization of the electrons.

4. Instantaneous cluster ionization: formation, equilibration and relaxation of a nano-plasma

Modeling instant ionization we assume for simplicity that all electrons absorb simultaneously one photon. Figure 4 shows the results for an Ar₅₅ cluster where one electron per atom was released at time $t = 0$ with an excess energy $E_0 = 4.24$ eV, according to a photon frequency $\hbar\omega = 20$ eV and the ionization potential of neutral argon $E_{\text{IP}} = 15.76$ eV; from that time on they are propagated classically. At the time of creation all electrons have positive energy and the cluster charge is equal to the cluster size as seen in figure 4(a). This corresponds to the temporary enhancements seen in figure 3 and discussed before. The value drops to about 0.2 similar to the values observed in the realistic calculations for Ar₁₃ and Ar₅₅. This drop is easily understood considering that the Coulomb energy of 55 singly-charged ions is larger than 3 keV. The total excess energy of the 55 electrons is, however, only about 233 eV. Thus for energetic reasons the majority of the electrons cannot leave the cluster volume.

More insight regarding the electron dynamics is gained by taking a closer look at the electron energies. Figure 4(b) shows separately the potential and kinetic energy of all quasi-free electrons. Their sum is approximately constant, violated only slightly through electrons which leave the cluster. This violation is small because, firstly, the number of electrons which leave the cluster during this time is negligible and, secondly, those which are lost carry only a very small amount of energy. Apparently there is an oscillatory exchange of potential and kinetic energy. The period of this oscillation is $\tau_{\text{osc}} \approx 0.79$ fs, which agrees with plasma period $\tau_{\text{pl}} = 2\pi/\omega_{\text{pl}} = \sqrt{\pi m/\rho e^2} = 0.77$ fs according to the atomic density ρ of argon at equilibrium structure³. Obviously those electrons which could not leave the cluster execute plasma oscillations.

² The ionization rate in figure 1(a) is considerably larger than in (c), which is somehow hidden by the different timescales.

³ The density is calculated for 55 atoms and a cluster radius of 8.5 Å. Atomic motion due to Coulomb explosion can be neglected on the considered time scale of a few femtoseconds.

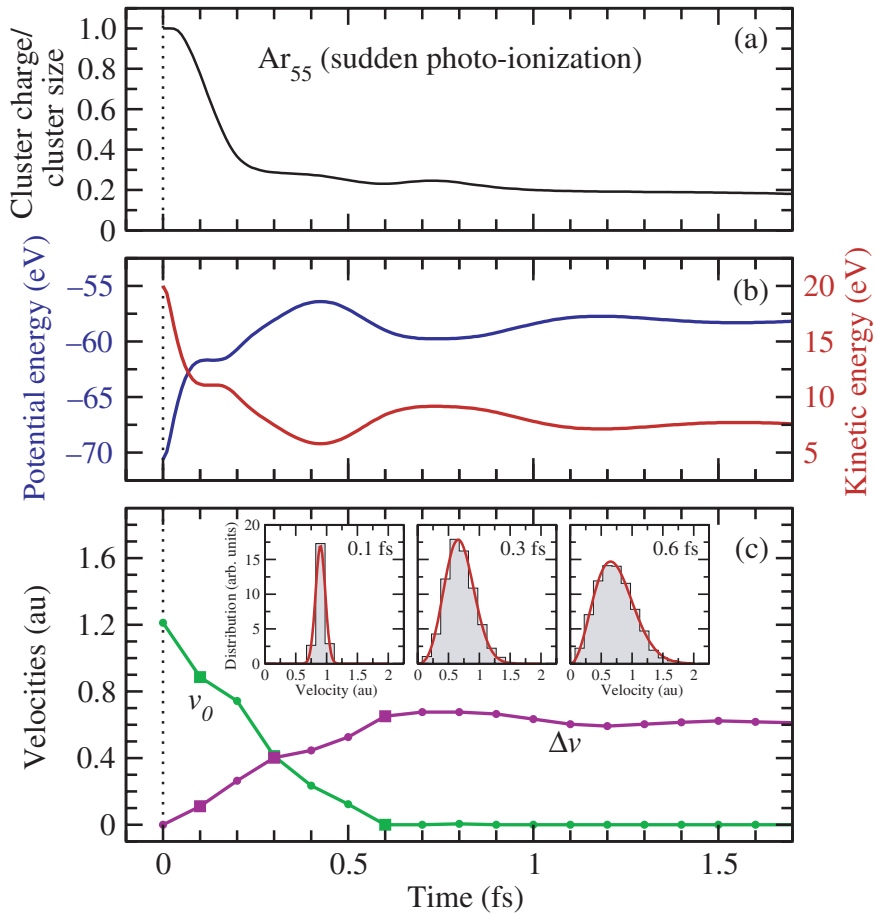


Figure 4. Time evolution after sudden single-photo-ionization of all atoms of an Ar_{55} cluster. From top to bottom: (a) total charge of the cluster divided by the cluster size, (b) potential (blue, right axis) and kinetic (red, left axis) energy of quasi-free electrons, i.e. electrons with negative energy, (c) fit parameter for the velocity distribution of equation (2). Insets: microscopic velocity distribution (gray-shaded bars) and corresponding fits (red lines) according to equation (2) for selected times (marked by squares).

That a plasma has formed on this short timescale may be surprising but can be seen in figure 4(c). For selected times, shown by dots in figure 4(c), we have calculated the velocity distribution of the quasi-free electrons. This distribution is fitted well for all times by the following function [10]:

$$f_{v_0, \Delta v}(v) = C v^2 \exp\left(-\frac{(v-v_0)^2}{\Delta v^2}\right), \quad (2)$$

with C an irrelevant normalization constant. The distribution of equation (2) contains both limits: monoenergetic electrons (with energy E_0) which corresponds to $v_0 = \sqrt{2E_0/m}$ and $\Delta v \rightarrow 0$ and an electron plasma at equilibrium (with temperature T) which corresponds to $v_0 = 0$ and $\Delta v = \sqrt{2kT/m}$. Hence, the ratio $v_0/\Delta v$ characterizes the degree of relaxation to equilibrium as a function of time. Starting with an infinitely large value at time $t = 0$ fs the

ratio vanishes around $t = 0.6$ fs. Thus in this finite plasma, the relaxation of the electronic distribution function takes about $\tau_{\text{rel}} = 0.6$ fs which is of the same order as the build-up of electronic correlations characterized by the plasma period $\tau_{\text{corr}} = 0.77$ fs. It is known from one-component plasmas [11] as well as from ultracold plasmas [12] that in this situation the plasma temperature undergoes oscillations about its equilibrium value if the plasma is strongly coupled, i.e. if the Coulomb-coupling parameter

$$\Gamma = \frac{E_{\text{pot}}}{E_{\text{kin}}} > 1, \quad (3)$$

with E_{pot} and E_{kin} the potential and kinetic energy of the quasi-free electrons, respectively. For the system studied here we find $\Gamma \approx 6$. The oscillations are damped out quickly in about two plasma periods which is typical for an inhomogeneous plasma [6]. Discussing kinetic and potential energy of the electrons as a function of time assumes that we have an ideal ‘probe’ of infinite time-resolution to record these energies. In the next section we discuss how close one can come to this ideal with attosecond pulses.

5. Creating and monitoring of non-equilibrium plasmas in clusters with attosecond pump–probe pulses

With today’s attosecond technology it is possible to come very close to the sudden excitation assumed in the previous section. If both the pump *and* the probe pulse have sub-femtosecond length, the non-equilibrium plasma oscillations can be observed by monitoring the time-dependent charging of the cluster as described in section 3. We have used pulse lengths of $\tau = 250$ as in order to ensure that the creation and probing of the plasma is fast on its timescale given by the plasma period of 770 as (see previous section). The pump intensity was chosen to induce on average the absorption of one photon per atom; thus most of the electrons are trapped by the cluster’s potential. The required intensities are not available yet, but intense attosecond sources are under active development [9]. The probing scenario is equivalent⁴ to that in section 3. We measure the kinetic energy of electrons kicked out by the probe pulse ($\hbar\omega = 150$ eV) as a function of the time delay. Thereby, we obtain the time-dependent charge which is close to the charge of the cluster if the pump pulse is short as discussed in section 3.

Figure 5 shows the probed charge (blue solid lines) for two pump laser frequencies $\hbar\omega = 20$ and 30 eV. In contrast to the scenario of section 3, the XUV photo-electrons originate exclusively from neutral or singly-charged argon. However, the dynamics of the surrounding plasma alters the cluster potential and, therefore, shows up in the kinetic energy of the photo-electrons. The plasma dynamics is revealed by the kinetic energy of the plasma electrons (red solid lines, cf red solid lines in figure 4(b)) giving evidence for oscillations, which are also reflected in the probing signal (blue solid lines). The oscillations become apparent after the initial energy drop during which the plasma formation occurs. They are more pronounced for the lower pump frequency (figure 5(a)) where on average one electron per atom is photo-ionized (blue dashed line). In the other case (figure 5(b)), with a lower electron density and longer plasma period, only one oscillation is visible. Similar to this *theoretical* quantity one observes a stronger contrast in the *measurable* probed charge for $\hbar\omega = 20$ eV than for $\hbar\omega = 30$ eV. These oscillations are solely

⁴ In contrast to the femtosecond pulses of section 3, one has to consider the large bandwidth of the attosecond pulse, which is taken into account by initiating the classical electron motion after photo-absorption with the corresponding energy spread.

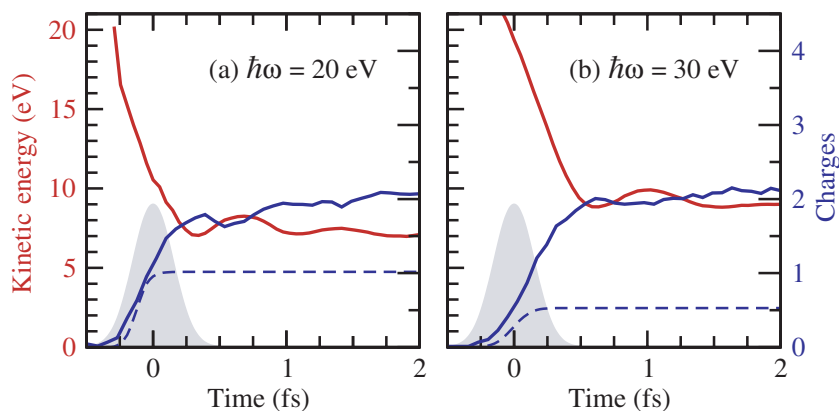


Figure 5. Time evolution after pumping of an Ar_{55} cluster by an attosecond VUV pulse (gray shaded areas) with duration $\tau = 250$ as, intensity $I = 5 \times 10^{14} \text{ W cm}^{-2}$ and (a) $\hbar\omega = 20$ eV or (b) $\hbar\omega = 30$ eV, respectively. The average kinetic energy (red lines, left axis) is shown along with the probed charge (solid blue lines, right axis). For completeness we show the ionic charges (dashed blue lines, right axis) which stay constant after the pulse.

due to the oscillating charge distribution; the ionic charges (blue dashed lines) remain constant after the pulse is over.

Although the nano-plasma generated by the attosecond pulse in the cluster differs by orders of magnitude in density, temperature and absolute number particles from an ultracold ‘micro’-plasma [13], we find very similar behavior for both finite plasmas, namely a fast decay of the plasma oscillations and more pronounced plasma oscillations for a larger Coulomb-coupling parameter Γ . In our case this is realized for 20 eV excitation frequency as compared to 30 eV, where for the former the density is higher (cf blue dashed lines in figure 5) and the temperature is lower (cf red lines in figure 5), hence the plasma is more strongly coupled. These observations are in accordance with the predictions from extended plasmas [11].

6. Summary

We have demonstrated that an attosecond pump–probe scheme opens the way to study non-equilibrium plasma phenomena in nano-plasmas created from finite systems such as rare-gas clusters. Initiated by a VUV pump pulse, the XUV probe pulse can map out the energy absorption of a finite multi-electron system—represented in our case by a small rare-gas cluster—*during* the creation of the electronic nano-plasma. Alternatively, the probe pulse can be used to trace the non-equilibrium dynamics of the plasma including its relaxation *after* its creation. In both cases, ultrafast photo-ionization of the cluster ions triggered by the probe pulse is used to determine the charging of the cluster which provides directly the information on energy absorption in the first case and on plasma oscillations indicative of non-equilibrium dynamics in the second case.

The fast timescale for the equilibration as well as the plasma oscillations indicate the formation of a strongly-coupled plasma which has been built up due to the high density of the cluster ions in combination with the relatively low energy of the electrons [14]. Hence, the

scheme proposed offers a route to make strongly-coupled plasmas in clusters experimentally accessible, which would boost our knowledge on dynamics in finite correlated multi-electron systems. With sufficiently high photon energies in the probe pulse such studies may be extended to larger clusters. The main limitation are inelastic collisions of the probing electron whereas the cluster charge is negligible here. These aspects will be investigated in more detail in future work.

References

- [1] Sansone G *et al* 2006 *Science* **314** 443
- [2] Drescher M, Hentschel M, Kienberger R, Uiberacker M, Yakovlev V, Scrinzi A, Westerwalbesloh T, Kleineberg U, Heinzmann U and Krausz F 2002 *Nature* **419** 803
- [3] Kienberger R *et al* 2004 *Nature* **427** 817
- [4] Georgescu I, Saalman U and Rost J M 2007 *Phys. Rev. Lett.* **99** 183002
- [5] Saalman U, Siedschlag C and Rost J M 2006 *J. Phys. B: At. Mol. Opt. Phys.* **39** R39
- [6] Pohl T, Pattard T and Rost J M 2005 *Phys. Rev. Lett.* **94** 205003
- [7] Georgescu I, Saalman U and Rost J M 2007 *Phys. Rev. A* **76** 043203
- [8] Cowan R D 1981 *The Theory of Atomic Structure and Spectra* (Berkeley, CA: University of California Press)
- [9] Krausz F 2007 private communication
- [10] MacDonald W M, Rosenbluth M N and Chuck W 1957 *Phys. Rev.* **107** 350
- [11] Zwicknagel G 1999 *Contrib. Plasma Phys.* **39** 155
- [12] Killian T C, Lim M J, Kulin S, Dumke R, Bergeson S D and Rolston S L 2001 *Phys. Rev. Lett.* **86** 3759
- [13] Killian T C, Pattard T, Pohl T and Rost J M 2007 *Phys. Rep.* **449** 77
- [14] Ramunno L, Jungreuthmayer C, Reinholz H and Brabec T 2006 *J. Phys. B: At. Mol. Opt. Phys.* **39** 4923